

# Polarization rotation induced by cascaded third-order processes

N. Minkovski, S. M. Satiel, and G. I. Petrov

*Faculty of Physics, University of Sofia, 5 J. Bourchier Boulevard, BG-1164, Sofia, Bulgaria*

O. Albert and J. Etchepare

*Laboratoire d'Optique Appliquée, Unité Mixte de Recherche 7639, Centre National de la Recherche Scientifique, Ecole Nationale Supérieure de Techniques Avancées–Ecole Polytechnique, Centre de l'Yvette, 91761 Palaiseau Cedex, France*

Received June 14, 2002

Intensity-dependent polarization rotation that results from the simultaneous action of two third-order processes, self-phase modulation and four-wave mixing, is observed. The effect is recorded along the fourfold axis of a YVO<sub>4</sub> crystal. The angle of rotation is proportional to the square of the input intensity–crystal length product. This is to the authors' knowledge the first experimental evidence showing that intensity-dependent polarization rotation can be related to the real part of cubic susceptibility. © 2002 Optical Society of America

OCIS codes: 190.0190, 190.3270, 190.4380, 190.4410, 190.4720, 230.5440.

In general, light propagating through a nonlinear medium experiences induced azimuth rotation (IAR) and induced ellipticity (IE).<sup>1,2</sup> If we restrict ourselves to nonlinear changes in the polarization state of nongyrotropic crystals, we can find in the literature<sup>1–6</sup> experimental and theoretical investigations that show that IAR is proportional to the imaginary part of  $\chi^{(3)}$  anisotropy, whereas IE is due to the real part of  $\chi^{(3)}$  anisotropy. On the basis of phase trajectory analysis, Dykman and Tarasov<sup>7</sup> showed that IAR can be observed also in nondissipative cubic crystals.

In this Letter we demonstrate, using a single-beam scheme, that at a high intensity level the real part of the cubic susceptibility is responsible not only for IE but also for induced changes in the polarization direction. The effect is interpreted in terms of cascaded third-order processes.

The experiment was performed with a single beam that propagates along the  $z$  axis of an yttrium vanadate (YVO<sub>4</sub>) crystal. This crystal belongs to the  $4/mmm$  symmetry point group, its  $z$  axis has fourfold symmetry, and it has no linear optical activity. The setup consists of a colliding-pulse mode-locking dye laser (maximum energy, 2  $\mu$ J; duration, 100 fs; frequency, 10 Hz; wavelength, 620 nm), an input polarizer, a 0.5-mm, (001)-cut YVO<sub>4</sub> crystal, and an output analyzer. The laser beam was focused on the sample with a 30-cm focal-length lens. The signals from two photodiodes, which measure input and output energies, are connected to a computer for signal averaging and processing. We measured the signal coming out of the sample sandwiched between the polarizer and the analyzer as a function of  $\beta$ , the angle of the input polarization plane with respect to the [100] axis of the crystal. For a polarizer and an analyzer that exactly cross, the signal measures the angle-dependent efficiency of the generation of cross-polarized waves (CPWs).<sup>8</sup> To study the output polarization state (consecutive to IE and IAR) we per-

formed extinction curve measurements by introducing small angular deviations  $\delta$  from the exact crossed position between the two polarizers. To analyze the sign of ellipticity we introduced a  $\lambda/4$  quartz plate with its  $c$  axis parallel to the input polarization in front of the analyzer. Furthermore, two-photon absorption and its anisotropy were estimated by measurement of the sample transmission for the same ensemble of  $\beta$  values.

The results of measuring the efficiency of XPW generation with a crossed polarizer and analyzer are shown in Figs. 1(a) and 1(b). Figure 1(a) shows the XPW rotational dependency. The maximum efficiency is at angles  $\beta = m\pi/4$  ( $m$  an odd number), consistently with the discussion in Ref. 5 and the theory described below. Figure 1(b) shows the quadratic intensity dependence of the XPW efficiency as measured at one of these maxima. Note that the XPW efficiency achieved is 1.2%, i.e., 3 orders of magnitude higher than in the experiments with  $\chi^{(2)}:\chi^{(2)}$  cascaded XPW generation in a  $\beta$ -barium borate crystal.<sup>8</sup> The reason for the good XPW efficiency in the YVO<sub>4</sub> experiment described here is the simultaneous matching of the wave vectors and group velocities along the  $z$  axis. With a longer crystal sample we can expect even higher XPW efficiency.

Typical results of extinction curve measurements are shown on Fig. 1(c) for three input intensities. The solid curves are parabolic fits of the type  $Y = C_1(\delta - \delta_0)^2 + C_2$ . The parameter  $\delta_0$  is a measure of the IAR angle, and  $|\epsilon| = \sqrt{C_2/C_1}$  is a measure of the modulus of IE. For the curve recorded at 0.96- $\mu$ J input energy the fit gives  $\delta_0 = +8.7$  mrad and  $|\epsilon| = 64$  mrad, and for the curve recorded at 1.83- $\mu$ J input energy the fit gives  $\delta_0 = +30$  mrad and  $|\epsilon| = 122.5$  mrad. The estimated accuracy for these parameters is 95%. An additional test with a  $\lambda/4$  plate proved that  $\epsilon < 0$ . Changes of angle  $\beta$  in increments of  $+\pi/4$  or  $-\pi/4$

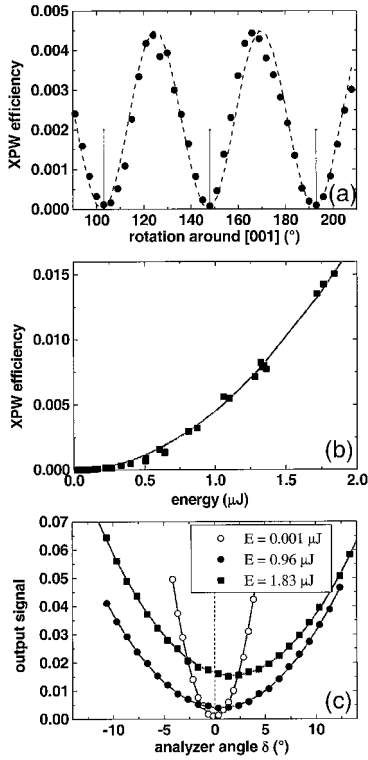


Fig. 1. (a) Evolution of a signal, through a crossed polarizer and analyzer, as a function of rotation of an  $\text{YVO}_4$  sample about its  $c$  axis. The vertical lines mark the angles where the input polarization is parallel to the [100], [110], or [010] axis. Dashed curve, a fit to the experimental points according to predictions of Eq. (6). (b) Variation of efficiency  $\eta = |B|^2/|A_0|^2$  as a function of input laser energy. The solid curve is a quadratic fit. (c) Analysis of the output signal (normalized to input intensity) with respect to angular detuning of the analyzer for three input energies  $E$ . Zero position corresponds to an exactly crossed polarizer and analyzer. Solid curves are parabolic fits according to relations (3).

lead to changes of sign for both  $\epsilon$  and  $\delta_0$ . The increase of the IE with input intensity is linear, in agreement with the theory.<sup>2,3</sup> If the observed IAR were the result of anisotropy in two-photon absorption, the intensity dependence of  $\delta_0$  would also be linear. Therefore we applied the procedure described in Ref. 9 to measure the amount of anisotropy of two-photon absorption. The result was  $0.01 \pm 20\%$  ( $0.02 \pm 20\%$ ) for an input energy of  $0.96 \mu\text{J}$  ( $1.83 \mu\text{J}$ ). On the basis of these data, we estimated that the IAR that is due to the anisotropy of the imaginary part of the cubic nonlinearity should be  $\delta_0 \approx 2 \text{ mrad}$  ( $4 \text{ mrad}$ ), far from the measured induced values of  $8.7 \text{ mrad}$  ( $30 \text{ mrad}$ ). In fact, measured IAR shows a quadratic dependence on input intensity, in great contrast to previous experiments.<sup>4</sup>

To describe the effect of IAR, let us consider, in the slowly varying envelope approximation, plane-wave propagation equations, neglecting linear absorption and choosing a coordinate system defined by the directions of the crossed polarizer and analyzer. The equations for self-phase modulation of copolarized component  $A$  and generation of XPWs with amplitude

$B$ , on the condition that  $|B| \ll |A|$  (i.e., if the possible effect on cross-phase modulation of wave  $A$  caused by the presence of wave  $B$  and self-phase modulation of wave  $B$  are neglected), are

$$dA/dz = i\gamma_{\parallel}|A|^2A, \quad dB/dz = i\gamma_{\perp}|A|^2A, \quad (1)$$

where  $\gamma_{\parallel} = \gamma_0[1 - (\sigma/2)\sin^2(2\beta)]$  and  $\gamma_{\perp} = -\gamma_0(\sigma/4)\sin(4\beta)$ ,  $\gamma_0 = (6\pi/\lambda n)\chi_{xxxx}^{(3)}$ , and  $\sigma$  is the anisotropy of the  $\chi^{(3)}$  tensor.<sup>1,10</sup> In general,  $\gamma_{\parallel} = \gamma_{\parallel}' + i\gamma_{\parallel}''$  and  $\gamma_{\perp} = \gamma_{\perp}' + i\gamma_{\perp}''$ . The solution to the system of Eqs. (1) with the initial conditions that  $B(0) = 0$  and  $A(0) = A_0$  ( $A_0$  real) is

$$A = A_0 \exp(i\gamma_{\parallel}A_0^2L), \quad (2a)$$

$$B = A_0(\gamma_{\perp}/\gamma_{\parallel})[\exp(i\gamma_{\parallel}A_0^2L) - 1]. \quad (2b)$$

Angle position  $\delta_0$  of the main ellipse axis and ellipticity angle  $\epsilon$  can be found by use of the equations<sup>11</sup>  $\tan(2\delta_0) = 2 \text{Re}(\Gamma)/(1 - |\Gamma|^2)$  and  $\sin(2\epsilon) = 2 \text{Im}(\Gamma)/(1 + |\Gamma|^2)$ , with complex parameter  $\Gamma = B/A$ . Alternatively, we may project the total output field ( $A, B$ ) onto the polarization plane of the analyzer that has deviated from the crossed position by angle  $\delta$ . The projected field is  $s(\delta) = -A \sin(\delta) + B \cos(\delta)$ . Let us neglect for a moment  $\gamma_{\perp}''$  and  $\gamma_{\parallel}''$ . Then the signal after the analyzer,  $S(\delta) = |s(\delta)|^2/A_0^2$ , will be

$$S(\delta) \approx \left[ \delta - \frac{2\gamma_{\perp}' \sin(\gamma_{\parallel}'A_0^2L/2)^2}{\gamma_{\parallel}'} \right]^2 + \left[ \frac{\gamma_{\perp}' \sin(\gamma_{\parallel}'A_0^2L)}{\gamma_{\parallel}'} \right]^2. \quad (3)$$

Equation (3) is derived with the assumption that the angle  $\delta$ ,  $\gamma_{\parallel}'A_0^2L$ , and  $\gamma_{\perp}'A_0^2L$  are small. The second term in expression (3) yields directly the square of ellipticity  $\epsilon^2$ ; the first term yields the IAR that is due to the real components of  $\chi^{(3)}$  tensor. We obtain

$$\delta_0 \approx 1/2 \gamma_{\perp}' \gamma_{\parallel}' A_0^4 L^2, \quad \epsilon^2 \approx (\gamma_{\perp}' A_0^2 L)^2. \quad (4)$$

A general analysis with complex  $\chi^{(3)}$  components gives

$$\delta_0 \approx -\gamma_{\perp}'' A_0^2 L + 1/2(\gamma_{\perp}' \gamma_{\parallel}' - \gamma_{\perp}'' \gamma_{\parallel}'') A_0^4 L^2, \quad (5a)$$

$$\epsilon^2 \approx [\gamma_{\perp}' A_0^2 L + 1/2(\gamma_{\perp}'' \gamma_{\parallel}' + \gamma_{\perp}' \gamma_{\parallel}'') A_0^4 L^2]^2. \quad (5b)$$

It is clear from relations (4) and (5) that the IE depends linearly on input intensity, whereas the IAR has a quadratic dependence when the anisotropy of the two-photon absorption, which is proportional to  $\gamma_{\perp}''$ , is small. Comparing relation (3) and the fits of the extinction curves shown in Fig. 1(c), we got for input energy  $0.96 \mu\text{J}$  ( $1.83 \mu\text{J}$ ) that  $\gamma_{\perp}' A_0^2 L = -0.063$  ( $-0.123$ ) and  $\gamma_{\parallel}' A_0^2 L = -0.270$  ( $-0.49$ ).

For a polarizer and an analyzer that cross exactly ( $\delta = 0$ ), from Eqs. (2) we obtain for the efficiency of XPW generation  $\eta = |B|^2/|A_0|^2$

$$\eta(2\gamma_{\perp}/\gamma_{\parallel})^2 \sin^2(\gamma_{\parallel}A_0^2L/2). \quad (6)$$

This expression for  $\eta$  explains the eightfold experimental dependence of the XPW generation shown in Fig. 1(a). Indeed, for  $|\gamma_{\parallel}A_0^2L| \ll 1$ , Eq. (6) becomes  $\eta \approx |\gamma_{\perp}|^2A_0^4L^2$ , and we note that  $\eta$  depends on the modulus of  $\gamma_{\perp}$  and on the square of intensity. The fit to the experimental points shown in Fig. 1(b) gives for energy 0.96  $\mu\text{J}$  (1.83  $\mu\text{J}$ ) the value  $|\gamma_{\perp}A_0^2L| = 0.064$  (0.121). The agreement between the value for  $|\gamma_{\perp}A_0^2L|$  obtained from the intensity curve for XPW generation and the value for  $\gamma_{\perp}'A_0^2L$  found from the extinction curves is additional proof that the imaginary part of  $\gamma_{\perp}$  is really small.

From relations (4) we see the role of the cascade processes. The expression for IAR angle  $\delta_0$  is proportional to  $\chi^{(3)}:\chi^{(3)}$ . The reason for cascaded rotation lies in the fundamental beam self-phase modulation effect experienced by fundamental wave  $A$ . At high input intensities the phase shift between  $B$  and  $A$  will be different from  $\pi/2$  and will be intensity dependent:  $\arg(\Gamma) = (\pi - \gamma_{\parallel}A_0^2L)/2$ , which will lead to a complex value of  $\Gamma$  and consequently to IAR. It is the cascading of efficient nonlinear self-phase modulation of the fundamental wave and the generation of a cross-polarized wave by four-wave mixing that cause the IAR. The effect described can be observed along crystallographic axes of cubic crystals or along the  $Z$  axes of tetragonal crystals. The condition for observing the effect is that  $\gamma_{\perp}''$  be small in combination with relatively high input intensity, such that  $\gamma_{\perp}''/(\gamma_{\perp}'\gamma_{\parallel}'A_0^2L) \ll 1$ . This condition is easy to satisfy when the fundamental photon energy is below half of the bandgap. In our experiment the fundamental photon energy is near the edge of half of the bandgap and the above inequality is well fulfilled because of the high intensity used.

The effect of  $\chi^{(3)}:\chi^{(3)}$  cascaded IAR is unique. This is not just a simple imitation of the effect of  $\chi^{(5)}$ . Indeed, if we consider nonlinear interaction owing to the real part of the inherent  $\chi^{(5)}$  components, the result will be an additional contribution to the IE but not to the IAR. Therefore, in contrast to most of the cascaded third-order effects (such as cascaded high-harmonic generation,<sup>12</sup> cascaded six-wave mixing,<sup>13-15</sup> and cascaded nonlinear phase shifts<sup>16</sup>) the effect of cascaded nonlinear polarization rotation reported here has no  $\chi^{(5)}$  analog.

Knowledge about this effect is important for avoiding unwanted depolarization effects. For example,  $\text{YVO}_4$  is known to be an active element for solid state lasers. Also, this effect can be used for measuring the magnitude and the sign of the components and therefore of the anisotropy of the tensor  $\chi^{(3)}$ . The attractive aspect of such a method lies in its

single-beam technique, with pumping and recording at the same wavelength; also, the measurement is based on recording values of angle rotation. However, if the cubic nonlinearity is known, measurement of the IAR angle can be used for calculating the intensity of the beam. Finally, polarization-switching devices similar to those proposed in Ref. 1 can be designed.

The project reported here was performed within Access to Research Infrastructure contract LIMANS III, CT-1999-00086. N. Minkovski, G. I. Petrov, and S. M. Saltiel thank the Laboratoire d'Optique Appliqué for its hospitality and support during their stay and also the Bulgarian Ministry of Science and Education for partial support from Science Foundation grant 803. S. M. Saltiel's e-mail address is saltiel@phys.uni-sofia.bg.

## References

1. W. A. Schroeder, D. S. McCallum, D. R. Harken, M. D. Dvorak, D. R. Andersen, A. L. Smirl, and B. S. Wherrett, *J. Opt. Soc. Am. B* **12**, 401 (1995).
2. Yu. P. Svirko and N. I. Zheludev, *Polarization of Light in Nonlinear Optics* (Wiley, New York, 1998).
3. M. G. Dubenskaya, R. S. Zadoyan, and N. I. Zheludev, *J. Opt. Soc. Am. B* **2**, 1174 (1985).
4. A. I. Kovrigin, D. V. Yakovlev, B. V. Zhdanov, and N. I. Zheludev, *Opt. Commun.* **35**, 92 (1980).
5. R. S. Zadoyan, N. I. Zheludev, and L. B. Meysner, *Solid State Commun.* **55**, 713 (1985).
6. A. D. Petrenko and N. I. Zheludev, *Opt. Acta* **31**, 1177 (1984).
7. M. I. Dykman and G. G. Tarasov, *Fiz. Tverd. Tela (Leningrad)* **24**, 2396 (1982) [*Sov. Phys. Solid State* **24**, 1361 (1982)].
8. G. I. Petrov, O. Albert, J. Etchepare, and S. M. Saltiel, *Opt. Lett.* **26**, 355 (2001).
9. A. A. Said, T. Xia, D. J. Hagan, E. W. Van Stryland, and M. Sheik-Bahae, *J. Opt. Soc. Am. B* **14**, 824 (1997).
10. M. D. Dvorak, W. A. Schroeder, D. R. Andersen, A. L. Smirl, and B. S. Wherrett, *IEEE J. Quantum Electron.* **30**, 256 (1994).
11. R. M. Azzam and N. M. Bashara, *Ellipsometry and Polarized Light* (North-Holland, Amsterdam, 1977).
12. A. Akhmanov, A. Dubovik, S. Saltiel, I. Tomov, and V. Tunkin, *Pis'ma Zh. Eksp. Teor. Fiz.* **20**, 264 (1974) [*Sov. Phys. JETP Lett.* **20**, 117 (1974)].
13. V. Astinov, K. J. Kubarych, C. J. Milne, and R. J. D. Miller, *Opt. Lett.* **25**, 853 (2000).
14. L. Misoguti, S. Backus, C. G. Durfee, R. Bartels, M. M. Murnane, and H. C. Kapteyn, *Phys. Rev. Lett.* **87**, 013601 (2001).
15. C. G. Durfee, L. Misoguti, S. Backus, H. C. Kapteyn, and M. M. Murnane, *J. Opt. Soc. Am. B* **19**, 822 (2002).
16. S. Saltiel, S. Tanev, and A. D. Boardman, *Opt. Lett.* **22**, 148 (1997).